

CLIP-Count: Towards Text-Guided Zero-Shot Object Counting

Ruixiang Jiang
rui-x.jiang@connect.polyu.hk
The Hong Kong Polytechnic
University
HKSAR, China

Lingbo Liu
lingbo.liu@polyu.edu.hk
The Hong Kong Polytechnic
University
HKSAR, China

Changwen Chen
changwen.chen@polyu.edu.hk
The Hong Kong Polytechnic
University
HKSAR, China

ABSTRACT

Recent advances in visual-language models have shown remarkable zero-shot text-image matching ability that is transferable to downstream tasks such as object detection and segmentation. However, adapting these models for object counting, which involves estimating the number of objects in an image, remains a formidable challenge. In this study, we conduct the first exploration of transferring visual-language models for class-agnostic object counting. Specifically, we propose CLIP-Count, a novel pipeline that estimates density maps for open-vocabulary objects with text guidance in a zero-shot manner, without requiring any finetuning on specific object classes. To align the text embedding with dense image features, we introduce a patch-text contrastive loss that guides the model to learn informative patch-level image representations for dense prediction. Moreover, we design a hierarchical patch-text interaction module that propagates semantic information across different resolution levels of image features. Benefiting from the full exploitation of the rich image-text alignment knowledge of pre-trained visual-language models, our method effectively generates high-quality density maps for objects-of-interest. Extensive experiments on FSC-147, CARPK, and ShanghaiTech crowd counting datasets demonstrate that our proposed method achieves state-of-the-art accuracy and generalizability for zero-shot object counting.

CCS CONCEPTS

• **Computing methodologies** → **Computer vision**; *Transfer learning*.

KEYWORDS

class-agnostic object counting, clip, zero-shot, text-guided

1 INTRODUCTION

Over the past decade, object-specific (e.g., crowd and vehicle) counting has been extensively studied [5, 11, 19–22, 28, 35, 39, 43, 45]. Despite the progress, it requires training a specific network with massively labeled samples for each class of objects. In contrast, the human counting ability is agnostic to specific object classes. When presented with previously unseen objects, we identify, compare, and treat similar objects as the counting target [2]. This observation has motivated the emerging development of class-agnostic object counting algorithms [3, 6, 15, 18, 24, 30, 37, 40, 49], which aim at training a unified/shared model to estimate the number of arbitrary objects-of-interest in the given image, as shown in Fig.1-(a). By annotating a few image patches as exemplars and computing the

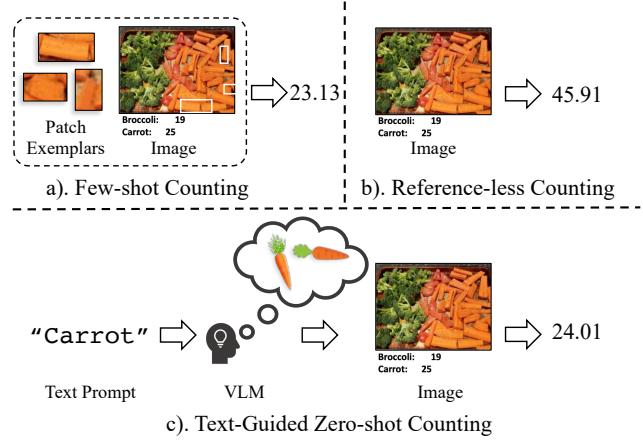


Figure 1: Illustration of different schemes of class-agnostic object counting. Specifically, few-shot counting requires manually-labeled image patches to specify the objects of interest, while reference-less counting mines and counts salient objects automatically, but it may fail to recognize objects of interest. In this work, we focus on the more flexible text-guided zero-shot counting, which uses text prompts to recognize and count objects of interest via Vision-Language Model (VLM), without relying on extra manual annotations.

similarities between exemplars and image regions, these methods have achieved good generalizability and counting accuracy.

However, most of previous class-agnostic counting methods assume that accurate bounding boxes of exemplars are easily available both during training and inference, which is not always the case in real-world applications. Therefore, in practice, they usually request users to manually annotate the exemplars of objects-of-interest, which is unfriendly to end-users. Moreover, even when exemplars are annotated, the high intra-class variance of query objects can still lead to biased object counts [18, 40]. To address these issues, reference-less methods have been proposed to automatically mine and count salient objects at inference time [6, 30]. While these approaches avoid cumbersome manual annotation, they lack the discriminative ability to specify the object class of interest in the presence of multiple object classes, as illustrated in Fig.1-(b). Overall, the limitations of existing counting schemes highlight the need for more flexible and robust guidance in generalized object counting.

In this work, we challenge the conventional notion that self-similarity between exemplars and image is essential for generalized object counting. To this end, we propose a new counting scheme

called text-guided zero-shot object counting, which utilize an additional natural language prompt as input to query object count in given images, as shown in Fig.1(c). In particular, the use of text prompts as guidance offers two main benefits. Firstly, it reduces the need for manual annotation of patch exemplars both during training and testing, making it more user-friendly and scalable to larger datasets. Secondly, text prompts offer greater flexibility compared to patch exemplars, as they can cover both general descriptions such as "food" and specific descriptions such as "red apple in a basket". Therefore, our text-guided scheme is more flexible and promising for class-agnostic object counting.

However, using natural language to guide generalized object counting presents several challenges. Firstly, unlike patch annotations that provide explicit appearance and shape information, text prompts only contain implicit descriptions of the query object, which can be intrinsically ambiguous. Additionally, text prompts are expected to precisely locate objects-of-interest in input images, and the effective semantic alignment of these two modalities is non-trivial. Moreover, achieving zero-shot object counting requires the model to be generalizable to open-vocabulary text prompts and object classes, but the lack of large-scale annotated datasets severely hinders the development and evaluation of text-guided zero-shot object counting methods.

Taking the above issues into consideration, we propose a unified text-guided zero-shot object counting method, termed **CLIP-Count**. Specifically, our method is developed based on Contrastive Language-Image Pre-training [29] (CLIP), which endows our model with zero-shot image-text alignment ability. To transfer the powerful image-level CLIP to dense tasks such as density estimation, we first design a patch-text contrastive loss to align text and patch embedding space. This alignment is achieved by simultaneously tuning visual [10] and text prompts [48, 49] to enable parameter-and-data-efficient transfer learning of pretrained CLIP. To propagate textual information to dense image feature for text-guided counting, we further elaborate a hierarchical patch-text interaction module that correlates text and image to different resolutions. Thanks to those tailor-designed modules, our method can effectively exploit the rich image-text alignment knowledge of CLIP to generate high-quality density maps for objects-of-interest. Extensive experiments on FSC-147 [31], CARPK [8], and ShanghaiTech [46] crowd count dataset demonstrate that our method is effective and generalizable to unseen object classes and text prompts.

In summary, our major contributions are as follows:

- To the best of our knowledge, our CLIP-Count is the first end-to-end text-guided zero-shot object counting model, which is flexible and scalable in real-world applications.
- We propose a novel approach whereby visual prompts and text prompts are learned simultaneously to fully exploit the rich pre-trained knowledge of CLIP.
- A patch-text contrastive loss is introduced to align text with dense visual features and improve the localization ability of CLIP for counting objects.
- Extensive experiments conducted on three object counting datasets demonstrate the state-of-the-art performance of the proposed CLIP-Count method.

2 RELATED WORKS

2.1 Few-shot Object Counting

Few-shot object counting algorithms aim to learn a generalized model that count anything with exemplar as inference-time guidance. The pioneering work, GMN [24] first formulate class-agnostic counting as a matching problem to exploit the self-similarity in counting task. Following this work, FamNet [31] learns to predict density maps with ROI pooling, and they further introduce a new dataset for class-agnostic counting, namely FSC-147 [31]. Subsequent improvements could be divided in two two streams. One approach is to employ more advanced visual backbones, such as vision transformers to enhance the extracted feature representation (e.g., CounTR [18], LOCA [3]). The second idea is to enhance the exemplar matching process by explicitly modeling exemplar-image similarity (e.g., BMNet [34], SAFECount [42]) or by further exploiting exemplar guidance [3, 17, 37]. Despite their good performance, all of those methods require additional patch-level annotation at training and inference time, which could be costly to obtain.

2.2 Reference-less and Zero-shot Object Counting

Reference-less counting has recently emerged as a more promising direction for class-agnostic counting without human annotation. The earliest attempts, RepRPN-Counter [30], proposes a region proposal module to extract the salient object in replace of exemplar input. RCC [6] leverages pretrained ViT [1, 4] to implicitly extract the salient objects, and directly regress a scalar as the estimated object count. Notably, some recent few-shot counting models [3, 18, 37] could also be configured to perform reference-less counting. While those methods do not need exemplars, they fail to provide a way for specifying object-of-interest in presence of multiple object classes. Concurrent with this work, Xu *et al.* [40] introduces the task of zero-shot object counting, where only the class name is needed in inference time. They employ a two-stage training scheme, where in the first stage they train a few-shot object counter with exemplar supervision. To achieve zero-shot counting, they additionally train a text-conditional variational autoencoder (VAE) on a close-set of objects for generating exemplar prototypes. Their work shares similarities with our proposed method at a high level. The key difference is that their two-stage training scheme still necessitates patch exemplars, and their method is limited by a closed-set of concepts. In contrast, our method does not require patch annotation at any stage and can be trained end-to-end, and we inherit the open-set prediction ability from CLIP.

2.3 Vision-Language Pre-training

VLMs pre-trained on extremely large dataset demonstrate advanced zero-shot image-text matching ability [9, 12, 29]. In particular, CLIP [29] learn an aligned multi-modal embedding space, and it has inspired various applications that use it as an image-level classifier [7, 27, 36, 44]. To further exploit the powerful image-level representation in CLIP to perform dense tasks, DenseCLIP [32] elaborate a context-aware prompting technique to facilitate dense prediction such as segmentation. Concurrently, RegionCLIP [47] identifies the lack of localization ability in CLIP, and they distill

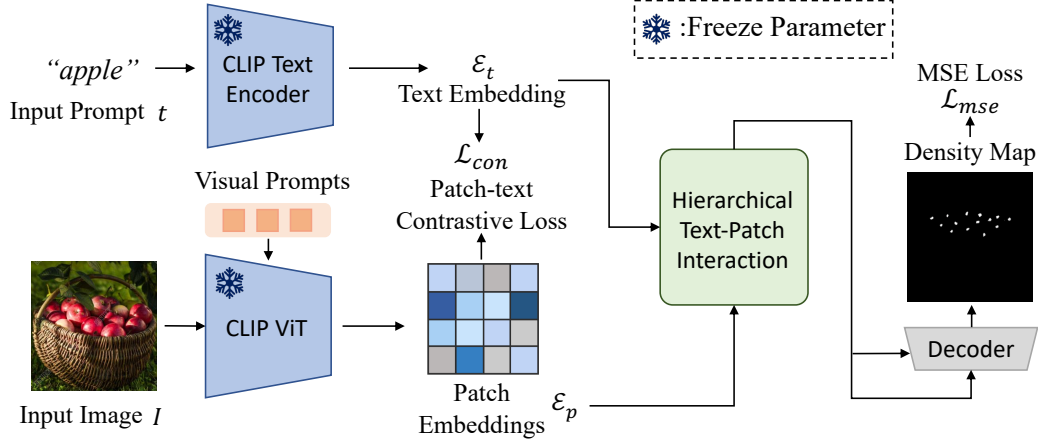


Figure 2: Overview of our CLIP-Count. We freeze both encoders in pretrained CLIP, and add a small amount of learnable prompts to transfer the pretrained knowledge. A patch-text contrastive loss is employed to align dense visual features with text. To interact the two modalities, we design a hierarchical text-patch interaction module that outputs multi-modal features at two resolutions. Finally, we decode the multi-modal feature maps with a decoder.

pre-trained knowledge in CLIP to enable fine-grained image-region matching. More recently, ZegCLIP [50] design a one-stage framework that calculate object masks based on patch embeddings, while GridCLIP [16] align grid-level representation with text to enable one-stage object detection. The majority of those improvements focus on segmentation and detection. Very recently, two CLIP-based object counting models were proposed [14, 26], both based on image-level classification and limited in counting granularity and accuracy. Currently, it remains a challenge to estimate a density map with CLIP.

3 METHOD

In this section, we present our proposed method, CLIP-Count, for text-guided zero-shot object counting. We will first review the structure of CLIP in Sec. 3.1. The objective of zero-shot class-agnostic object counting is defined in Sec. 3.2. We elaborate on the design of our proposed method in Sec. 3.3, and Sec. 3.4.

3.1 Preliminary: CLIP

CLIP [29] connects image and language through large scale pre-training on image and text pairs. It learns to align the text and image representations, so that the similarity of an image and text pair could be calculated by dot product of their respective embeddings. Formally, let $\mathcal{E}_I \in \mathbb{R}_n$ and $\mathcal{E}_t \in \mathbb{R}_n$ denote the embedding of an image I and a text t , where $n = 512$ is the dimension of CLIP embedding space. The cosine similarity of the text and image pair could be calculated as:

$$\text{CLIP}(I, t) = \frac{\mathcal{E}_t \cdot \mathcal{E}_I}{\|\mathcal{E}_t\| \|\mathcal{E}_I\|} \quad (1)$$

CLIP employs two encoders for encoding the image and text. Specifically, the last layer of ViT-based CLIP visual encoder [4] outputs a global image feature $z_0 \in \mathbb{R}_d$ and a 1/16 resolution patch-level feature map $z_x \in \mathbb{R}_{p^2 \times d}$, where $p = 14$ denotes the number of image patches per column and row, and $d = 768$ represents ViT latent dimension. CLIP applies a linear projection $\phi_z : \mathbb{R}_d \mapsto \mathbb{R}_n$

over the global feature to get the image embedding $\mathcal{E}_I = \phi_z(z_0)$, while the patch-level feature map z_x is discarded. In this work, we focus on utilizing z_x for density estimation.

3.2 Objective

Our objective is to count anything with text guidance. Formally, given an image $I \in \mathbb{R}_{H \times W \times 3}$ that contains arbitrary object classes, as well as a natural language prompt t that specifies the object(s) of interest, our objective is to estimate a density map $\hat{y} \in \mathbb{R}_{H \times W}$ for the specified object(s). The estimated object count could be calculated by summing the density map $N_{pred} = \text{SUM}(\hat{y})$.

Under the class-agnostic setting, we denote the object classes contained in each set as $C_{train}, C_{val}, C_{test}$. The testing and validation sets do not overlap with the training set: $C_{train} \cap C_{val} = \emptyset$ and $C_{train} \cap C_{test} = \emptyset$. We optimize the model $F_\theta(I, t) = \hat{y}$ on the training set using ground truth density map supervision y , and evaluate its performance on the validation and testing sets.

It is worth noting that incorporating text guidance at inference time is a standard practice both for zero-shot object counting [40] and for other text-driven tasks with CLIP [7, 33, 36, 50]. Additionally, previous research [3, 6, 18] use the terms “reference-less counting” and “zero-shot counting” interchangeably, despite their inherent differences. For clarity, we refer to the methods that solely utilize image input as “reference-less”, while those that incorporate text as guidance are referred to as “zero-shot counting”. Fig. 1 summarizes their difference.

3.3 Aligning Text with Dense Visual Features

CLIP has demonstrated remarkable performance in measuring global image-text similarity. However, transferring such ability to pixel level for dense-prediction is non-trivial, as the vanilla CLIP intrinsically lacks localization ability [32], which limits its performance in object detection, segmentation, and counting. To alleviate this limitation, we propose adapting the CLIP vision encoder to enhance the localization ability of patch-level feature map z_x .

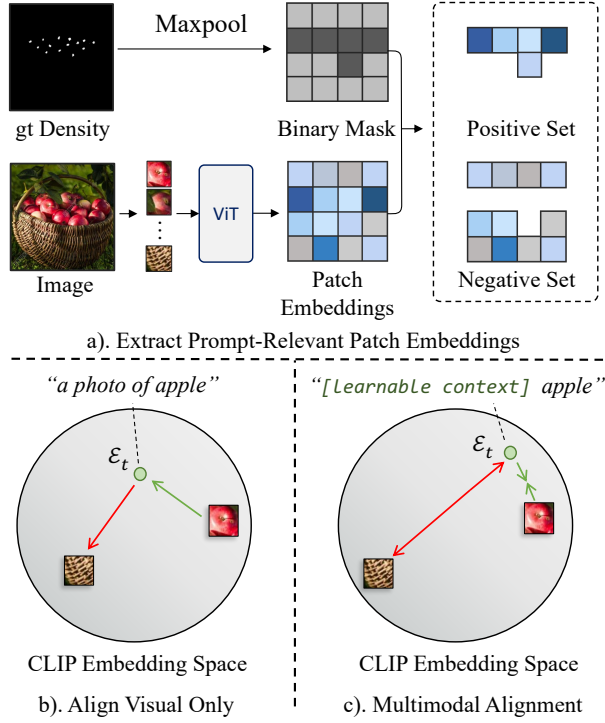


Figure 3: Illustration of Patch-Text Contrastive Loss. a.) we utilize the ground truth density map to determine the objectness at patch-level, and we split the patch embeddings into two sets accordingly; b.) finetune the visual encoder to align patch embeddings to the fixed text embedding space; c.) shift both text and patch embeddings. The number of patches in a) and the two image patches in b) and c) are only for illustration purposes.

To be more specific, we propose a patch-text contrastive loss that maximizes the mutual information between text prompt and prompt-relevant patch-level features. To achieve this, we first apply a linear projection to map the feature map to the same dimension as the text embedding \mathcal{E}_t :

$$\{\mathcal{E}_p^i = \phi_p(z_x^i) | i = 0, 1, \dots, p^2\} \quad (2)$$

For brevity, we call the reshaped $\mathcal{E}_p \in \mathbb{R}_{p \times p \times n}$ as *patch embeddings* of the input image. It is worth noting that this naming differs from the convention used in ViT, as our \mathcal{E}_p encodes cross-patch information due to the image-level perceptive field in global attention [4]. To determine the location of objects, we apply maxpooling to the ground truth density map y to get a patch-level binary mask for objectness. We then define \mathcal{P} and \mathcal{N} as the positive and negative sets of patch embeddings, respectively, depending on their corresponding mask value. Similar as CRIS [38], we introduce the following InfoNCE-based [25] contrastive loss:

$$\mathcal{L}_{con} = -\log \frac{\sum_{i \in \mathcal{P}} \exp(s(\mathcal{E}_p^i, \mathcal{E}_t)/\tau)}{\sum_{i \in \mathcal{P}} \exp(s(\mathcal{E}_p^i, \mathcal{E}_t)/\tau) + \sum_{k \in \mathcal{N}} \exp(s(\mathcal{E}_p^k, \mathcal{E}_t)/\tau)} \quad (3)$$

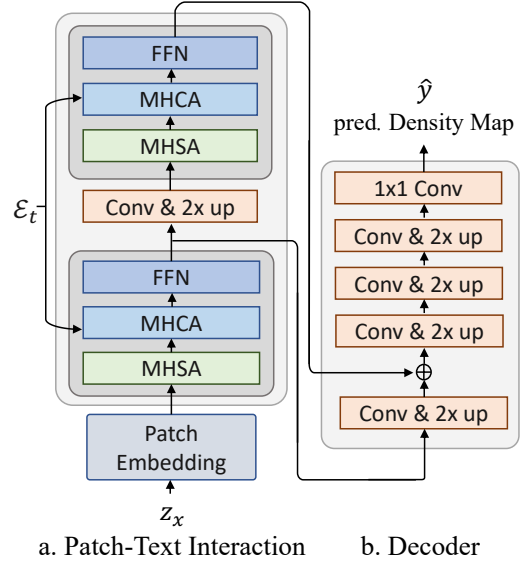


Figure 4: Architecture of the proposed Hierarchical Patch-Text Interaction Module and Decoder. For brevity, we omit the normalization layers, positional encoding, and activation functions.

where $s(.,.)$ denotes cosine similarity, and $\tau = 0.07$ is the temperature parameter [25]. The contrastive loss function in Eqn. 3 aligns the patch embedding space with the text embedding space by pulling positive patch embeddings closer to the fixed text embedding and pushing negative patches further away, similar to the pre-training objective of CLIP[29]. We also find it beneficial to adjust both the patch and text embeddings simultaneously, as the prompt templates used by CLIP such as “a photo of [class]” typically describe the image as a whole, rather than at the patch level. Inspired by CoOp [49], we optimize continuous token embeddings as the context of input prompt in an end-to-end manner. The entire procedure is summarized in Fig. 3.

3.4 Adapting CLIP for Density Estimation

Our patch-text contrastive loss is designed to enhance the patch-level representation and improve the localization ability of CLIP. Nonetheless, two key questions remain: 1) how to finetune the visual encoder, and 2) how to decode the patch-level feature map into a text-conditional density map. In this section, we address these questions.

Visual Prompt Tuning. Our model involves transferring the pretrained knowledge in CLIP visual transformer for dense prediction. However, the conventional “pre-training + finetuning” paradigm would be computationally expensive as it requires updating the entire model. Furthermore, finetuning a transformer usually requires a significant amount of data, which may not be practical when annotations are expensive to obtain, as is often the case with object counting. To effectively exploit the pretrained knowledge in CLIP, we instead freeze the parameters in CLIP ViT, and concatenate a small amount of trainable parameters as visual prompts [10] to the input of each transformer layer. This allows us to transfer

the knowledge in CLIP using a much smaller amount of data and memory while still benefiting from the rich visual representation learned in CLIP. We refer readers to the original paper on Visual Prompt Tuning (VPT) [10] for further details.

Hierarchical Text-Patch Interaction Module. Visual features usually span a variety of scales, yet the transformer structure intrinsically lacks the inductive bias for modeling scale-invariant features [13], resulting in inaccurate density estimation. To address this issue, we propose a lightweight hierarchical transformer with cross-attention to enable the propagation of text information to different scales of the image feature. Our interaction module comprises two similar layers, where each layer sequentially applies multihead self-attention (MHSA), multihead cross-attention (MHCA), and a two-layer MLP (FFN). The MHSA captures long-distance relationships, while the MHCA propagates semantic information embedded in text to visual features. In between the two layers, a convolution layer with a skip connection is employed, followed by a $2\times$ bi-linear interpolation layer that doubles the resolution of the internal multimodal feature map $M_c \in \mathbb{R}_{p \times p \times n}$. The motivation is to capture the relationship between text and image at a finer granularity [13]. The final output of the interaction module are the coarse M_c and fine $M_f \in \mathbb{R}_{2p \times 2p \times n}$ multi-modal feature maps. We limit the number of scales to two, as we find that this design provides the best balance between cost and performance. The entire process is visualized in Fig 4-(a).

Density Map Regression. We decode the multi-modal feature maps M_c and M_f using a CNN-based decoder, as illustrated in Fig 4-(b). The decoder consists of several convolutional blocks and $2\times$ interpolation layers that sequentially increase the spatial resolution and decrease the channel dimension in each layer. To decode the two-scale feature maps from the interaction module, we first perform convolution on the coarse multi-modal map M_c , and fuse it with M_f before the second convolution by summation:

$$M'_f = \text{Lerp}(\sigma(\text{Conv}_{3 \times 3}(M_c))) + \sigma(\text{Conv}_{1 \times 1}(M_f)) \quad (4)$$

where $\text{Lerp}(\cdot)$ denotes bi-linear interpolation, $\sigma(\cdot)$ is the activation function. The final output of the decoder is obtained through a 1×1 convolution layer with sigmoid activation.

4 EXPERIMENTS

4.1 Dataset

FSC-147. FSC-147 [31] is a dataset recently proposed for class-agnostic object counting. It consists of 6,135 images across 147 object classes, with non-overlapping object classes in each set. For each training image, the dataset provides its class name, dot supervision, and three random bounding boxes of objects (i.e. the exemplar patch annotation). In our experiments, we use the class name as the text prompt t , and do not use the patch annotation.

CARPK. CARPK [8] provides 1448 birds-eye view image of parking lots, containing a total of 89,777 cars. We use CARPK to evaluate the cross-dataset transferability of our model.

ShanghaiTech. The ShanghaiTech crowd counting dataset [46] is a comprehensive dataset for crowd counting. It comprises two parts, A and B, with a total of 1,198 annotated images. Part A consists of 482 images, with 400 designated for training and 182 for testing. Part B comprises 716 images, with 400 for training and 316

for testing. Notably, the two parts were collected using different methods, which presents a challenge for cross-part evaluation.

4.2 Implementation Details

Architecture Detail. We use OpenAI CLIP with ViT-B/16 backbone. For the visual encoder, we use deep version of VPT, with 15 visual prompts in each layer. For context learning, we use 2 prefix tokens. For density decoder, we use 3×3 convolution kernel with stride = 1 and padding = 1 to keep spatial resolution. GeLU non-linearity is used after each convolution layer.

Training Detail. The model is trained on the training set of FSC-147. We view our proposed contrastive loss as a pretext task to improve feature representation. Therefore, we pre-train the model with contrastive loss for 30 epochs before further training it with mean square error (MSE) loss only for 200 epochs using the AdamW [23] optimizer. The MSE loss is defined as:

$$\mathcal{L}_{MSE} = \frac{1}{H \times W} \|y - \hat{y}\|^2 \quad (5)$$

During both training stages, we use a batch size of 32 and a learning rate of 1×10^{-4} , which decays by a factor of 0.33 after 100 epochs. The whole training process takes approximately 3 hours on a single RTX-3090Ti GPU. We apply the same data augmentations as used in CounTR [18], except for their proposed mosaic augmentation. Additionally, to comply with the input assumption of CLIP, we downsample the training images to 224×224 , whereas previous generalized counting methods on FSC-147 typically use a resolution of 384×384 .

4.3 Evaluation Metric

Following previous class agnostic counting methods [3, 6, 18, 31, 40], we evaluate the performance by mean absolute error (MAE) and root mean squared error (RMSE).

$$\text{MAE} = \frac{1}{N_I} \sum_{i=1}^{N_I} |N_{pred}^i - N_{gt}^i|, \quad (6)$$

$$\text{RMSE} = \sqrt{\frac{1}{N_I} \sum_{i=1}^{N_I} (N_{pred}^i - N_{gt}^i)^2} \quad (7)$$

where N_I denotes the number of images in testing set, and N_{pred} , N_{gt} is the predicted and ground truth object counts.

5 RESULT AND ANALYSIS

5.1 Quantitative Result

To the best of our knowledge, this is the first study to investigate the application of VLMs for zero-shot density map regression in both generalized counting and class-specific counting settings. As such, a direct comparison with previous methods is impractical. To evaluate the performance of our approach, we compared it to several state-of-the-art few-shot and reference-less generalized object counting methods, including FamNet [31], CFOCN [41], CounTR [18], LOCA [3], RepRPN-C [30], RCC [6], and the only other zero-shot counting method [40] on FSC-147. Additionally, we compared our model with class-specific counting models on the CARPK and ShanghaiTech crowd counting datasets, in a cross-dataset setting.

Table 1: Comparison with State-of-the-art Methods on FSC-147. (*) denotes adopting modification for reference-less counting as described in RCC [6]. We highlight the best result for each scheme in bold.

Scheme	Method	Source	#Shot	Val Set		Test Set	
				MAE	RMSE	MAE	RMSE
Few-shot	FamNet [31]	CVPR2021	3	24.32	70.94	22.56	101.54
	CFOCNet [41]	WACV2021	3	21.19	61.41	22.10	112.71
	CounTR [18]	BMVC2022	3	13.13	49.83	11.95	91.23
	LOCA [3]	arXiv2022	3	10.24	32.56	10.97	56.97
	FamNet [31]	CVPR2021	1	26.05	77.01	26.76	110.95
Reference-less	FamNet* [31]	CVPR2021	0	32.15	98.75	32.27	131.46
	RepRPN-C [30]	ACCV2022	0	29.24	98.11	26.66	129.11
	CounTR [18]	BMVC2022	0	18.07	71.84	14.71	106.87
	LOCA [3]	arXiv2022	0	17.43	54.96	16.22	103.96
	RCC [6]	arXiv2022	0	17.49	58.81	17.12	104.53
Zero-shot	Xu <i>et al.</i> [40]	CVPR2023	0	26.93	88.63	22.09	115.17
	Ours	-	0	18.79	61.18	17.78	106.62

Table 2: Cross-Dataset Evaluation on CARPK Dataset. (*) Trained using same backbone with ours.

Method	#Shot	MAE	RMSE
FamNet [31]	3	28.84	44.47
BMNet [34]	3	14.41	24.60
BMNet+ [34]	3	10.44	13.77
RCC* [6]	0	21.38	26.15
Ours	0	11.96	16.61

Table 3: Cross-Dataset Evaluation on ShanghaiTech Crowd Counting Dataset. (*) Trained using same backbone with ours.

Method	Type	Training→Testing	MAE	RMSE
MCNN [46]	Specific	Part A→Part B	85.2	142.3
CrowdCLIP [14]			69.6	80.7
RCC* [6]	Generic	FSC147→Part B	66.6	104.8
Ours			45.7	77.4
MCNN [46]	Specific	Part B→Part A	221.4	357.8
CrowdCLIP [14]			217.0	322.7
RCC* [6]	Generic	FSC147→Part A	240.1	366.9
Ours			192.6	308.4

Quantitative Result on FSC147. We compare CLIP count with state-of-the-art class-agnostic object counting methods on FSC-147 and summarize the quantitative result in Tab. 1. Overall, we outperform the state-of-the-art zero-shot object counting method [40] on the FSC-147 dataset. We also compare our results with those of few-shot and reference-less methods for reference. It is worth noting that zero-shot object counting aims to solve a more challenging scenario compared to few-shot counting and reference-less counting, as the model needs to understand the relationship between semantic information and visual features.

Quantitative Result on CARPK. Following previous class-agnostic counting methods [6, 24, 34], we test CLIP-Count on CARPK to evaluate its cross-dataset generalizability. Specifically, the model is trained on FSC-147 and evaluated on the testing set of CARPK without fine-tuning. To ensure a fair comparison, we train RCC with the same visual backbone (i.e., ViT-B/16) on FSC-147, instead of their proposed FSC-133. As shown in Tab. 2, our approach outperforms the representative reference-less counting method, RCC, by a significant margin.

Quantitative Result on ShanghaiTech Concurrent with this work, Liang *et al.* [14] propose the first CLIP-based crowd counting method, namely CrowdCLIP. In their paper, they evaluate the cross-dataset performance of models by training the class-specific models on one part of the ShanghaiTech dataset and test them on another. We conduct a similar experiment by directly evaluating our model and RCC [6] for crowd counting (i.e., no finetuning on any part of ShanghaiTech). Similar as the experiment on CARPK, we also modified the backbone of RCC to ensure fairness. The results are summarized in Tab. 3. Our proposed generic counting method outperforms the representative class-specific counting methods MCNN [46] and CrowdCLIP [14] by a significant margin, even without training on any part of the crowd-counting dataset. In particular, we outperform CrowdCLIP by 11.2%, 4.0%, 34.3%, and 3.7% under cross-dataset setting. Moreover, our method significantly outperforms the other reference-less counting method, RCC [6]. Overall, the experiment demonstrate the advanced cross-dataset generalizability of CLIP-Count.

5.2 Qualitative Result

We visualize qualitative results in Fig. 5, where we overlay predicted density map on the input image. We provide a side-by-side comparison with our method against the state-of-the-art zero-shot method [40] in Fig. 5(a), and few-shot method, LOCA [3], in Fig. 5(b) on the FSC-147 dataset. Compared with [40], our proposed method could better localize high density in the center of the object with high-fidelity. By contrast, the density prediction in [40]

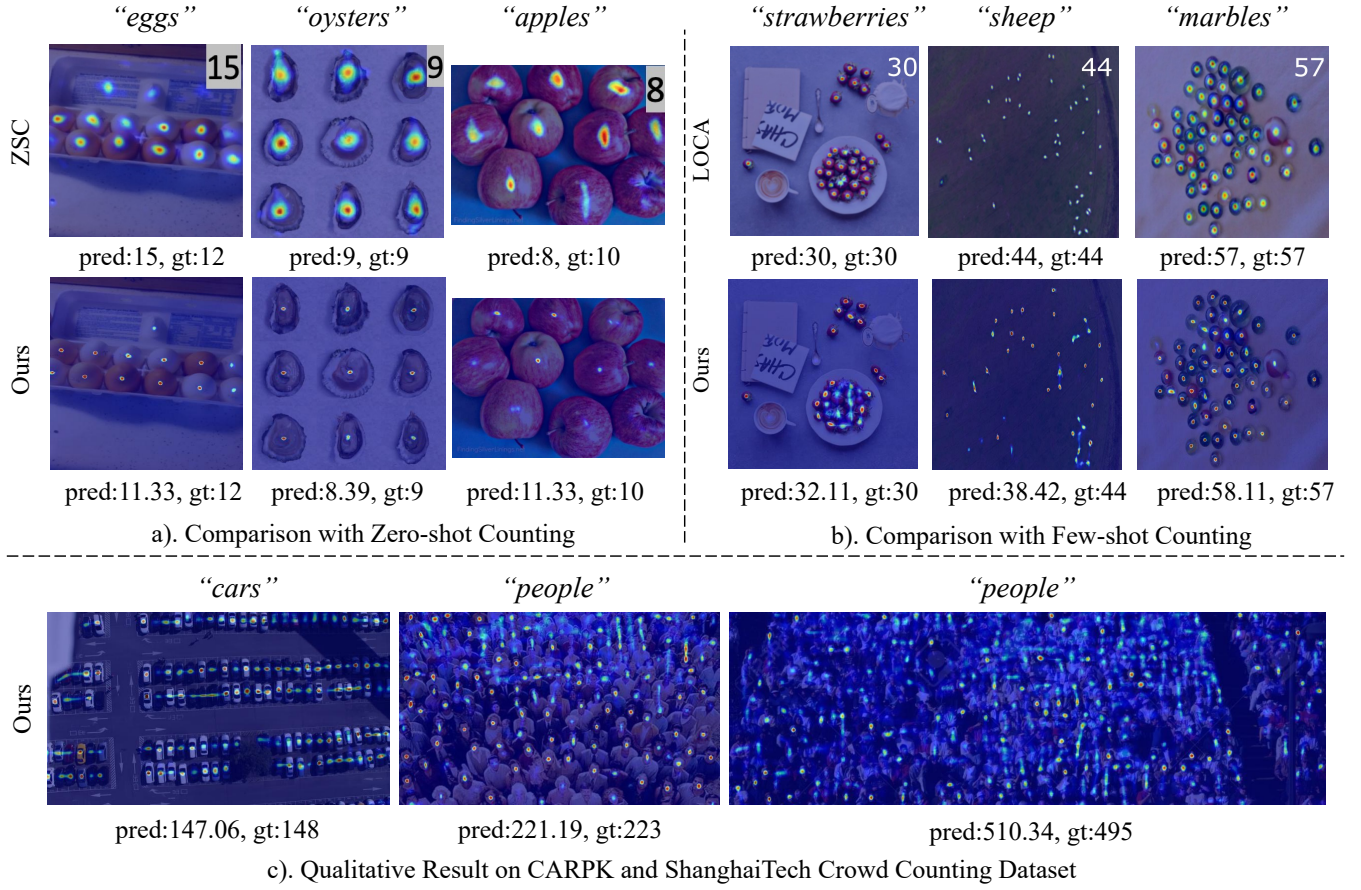


Figure 5: Qualitative Result. We compare CLIP-Count with the state-of-the-art zero-shot [40] and few-shot counting method [3] on FSC-147 in a) and b). In c) we visualize results on the CARPK and ShanghaiTech datasets.

Table 4: Ablate Study. We show the number of trainable parameters and the evaluation metrics on FSC-147 dataset.

Method	Interaction	Transfer	Contrastive	#Param.	Val Set		Test Set	
					MAE	RMSE	MAE	RMSE
A1	Add	Freeze	None	3.3M	30.40	96.67	33.84	124.64
A2	Naive	Freeze	None	16.0M	32.50	95.02	31.48	121.95
A3	2-Scale	Freeze	None	16.6M	29.96	93.07	28.84	120.03
B1	2-Scale	Finetune	None	102 M	24.88	77.73	22.51	131.12
B2	Naive	VPT	None	16.6M	20.43	69.26	19.26	108.71
B3	2-Scale	VPT	None	17.3M	20.01	66.08	18.77	108.00
C1	2-Scale	VPT	Visual	17.3M	19.21	64.93	18.55	107.51
C2	2-Scale	VPT	Multi-modal	17.3M	18.79	61.18	17.78	106.62

exhibits non-concentrated patterns. Our model could also achieve similar results with the representative few-shot counting method, both in terms of prediction error and fidelity of density map. We also visualized a few high-density images from the CARPK and ShanghaiTech datasets.

5.3 Ablation Study

We validate the design choices of CLIP-Count by conducting extensive ablation experiments. Our baseline model (A1) is frozen CLIP with a CNN-decoder only. Based on this, we iteratively add components with different designs. Specifically, we have experimented with the following three design choices: (A) how to interact

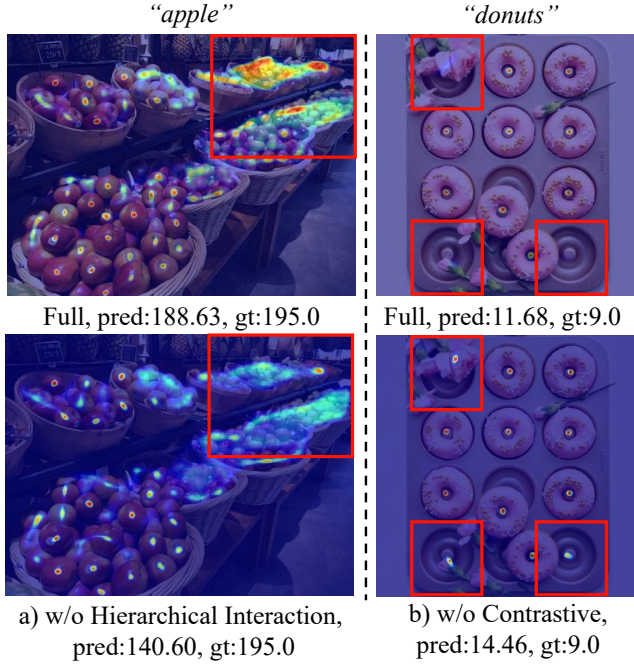


Figure 6: Visualization of Ablation Study. a) Replace the hierarchical interaction with a plain transformer; b) Remove the contrastive loss.

multi-modal features (B) how to fine-tune CLIP ViT, and (C) the effect of patch-text contrastive loss. For (A), “*add*” means add text embedding to patch embeddings, “*naïve*” means use a plain vision transformer [4, 18] without hierarchical design; for (B) “*finetune*” means finetune all ViT parameters; for (C) Contrastive loss, “*visual*” means adjust patch embeddings only, and “*multimodal*” means adjust text and patch embeddings at the same time. We summarize the results in Tab. 4, and we also visualize the effect of hierarchical interaction and contrastive loss in Fig. 6.

The proposed designs effectively improve the performance of the model in generalized object counting tasks. The cross-attention mechanism outperforms baseline in modeling complex text-image relationships. The hierarchical design of the interaction module helps the model handle size variations of objects, such as the example in Fig. 6-(a). Additionally, the VPT enables parameter-and-data-efficient transfer learning by adding a small amount of trainable visual prompts, bringing 19.5% and 14.5% gain in MAE and RMSE, respectively, with only 3% of additional parameters. The contrastive loss guides the model to fill the gap between text and dense image features, leading to 6.1% and 7.6% improvements for both metrics. Without the contrastive loss, the model would mistakenly treat visually similar objects as “*donuts*,” as shown in Fig. 6-(b).

5.4 Limitations and Future Works

Despite its promising results, CLIP-Count may encounter limitations in certain scenarios due to the inherent ambiguity in text guidance for object counting. Two representative examples of such cases are visualized in Fig. 7. Specifically, in (a), the prompt “*apple*”

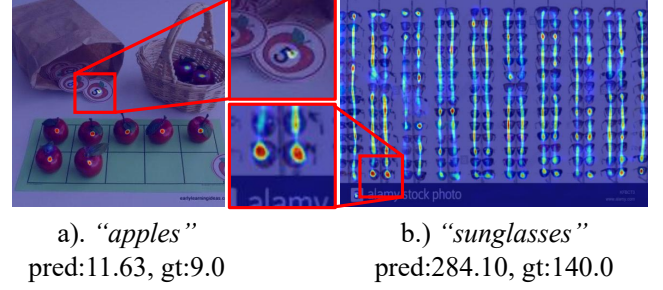


Figure 7: Representative Failure Cases of CLIP-Count.

can refer to either the fruit or a drawing of an apple, presenting a case of semantic ambiguity. In face of linguistic ambiguity like this, our model may produce unwanted results. Another example is shown in Fig. 7-(b), where the queried object itself could be ambiguous, as the “*sunglasses*” consists of two similar components (i.e., two lenses). While the ground truth treats the whole pair as one object, our model counts them separately, resulting in a doubled count. We attribute these limitations to the inadequate prompt annotation in FSC-147, where only a general class name is available for text guidance. In future work, we plan to focus on collecting a dataset with more fine-grained text annotation to disambiguate the query object and enhance model accuracy.

6 CONCLUSION

This paper presents CLIP-Count, a novel generalized object counting method that leverages text guidance to achieve zero-shot generalized object counting. The proposed method leverages the recently proposed visual-language model, CLIP, to enable zero-shot image-text matching. To transfer image-level CLIP for dense tasks, a patch-text contrastive loss is introduced to align text with dense visual features, enabling parameter-and-data-efficient transfer of pre-trained knowledge in CLIP to the task of dense prediction through visual prompt tuning. The model also involves a hierarchical patch-text interaction module to interact text and visual feature at different resolutions, followed by a CNN-based decoder. Experimental results on the FSC-147 dataset demonstrate that our method outperforms the current state-of-the-art zero-shot generalized counting method. Further experiments on the CARPK and ShanghaiTech crowd counting datasets further demonstrate the generalizability of proposed method in a cross-dataset setting. We have also experimented with the key design choices in CLIP-Count and demonstrated the effectiveness of our design. However, failure cases are observed, particularly due to inherent ambiguity in text, and we suggest future research focus on establishing a counting dataset with fine-grained text annotations.

REFERENCES

- [1] Mathilde Caron, Hugo Touvron, Ishan Misra, Hervé Jégou, Julien Mairal, Piotr Bojanowski, and Armand Joulin. 2021. Emerging properties in self-supervised vision transformers. In *Proceedings of the IEEE/CVF international conference on computer vision*. 9650–9660.
- [2] Stanislas Dehaene. 2011. *The number sense: How the mind creates mathematics*. OUP USA.
- [3] Nikola Djukic, Alan Lukezic, Vitjan Zavrtanik, and Matej Kristan. 2022. A Low-Shot Object Counting Network With Iterative Prototype Adaptation. *arXiv*

- preprint arXiv:2211.08217 (2022).
- [4] Alexey Dosovitskiy, Lucas Beyer, Alexander Kolesnikov, Dirk Weissenborn, Xi-aohua Zhai, Thomas Unterthiner, Mostafa Dehghani, Matthias Minderer, Georg Heigold, Sylvain Gelly, et al. 2020. An image is worth 16x16 words: Transformers for image recognition at scale. *arXiv preprint arXiv:2010.11929* (2020).
 - [5] Tao Han, Lei Bai, Junyu Gao, Qi Wang, and Wanli Ouyang. 2022. Dr. vic: Decomposition and reasoning for video individual counting. In *Proceedings of the IEEE/CVF Conference on Computer Vision and Pattern Recognition*. 3083–3092.
 - [6] Michael Hobley and Victor Prisacariu. 2022. Learning to Count Anything: Reference-less Class-agnostic Counting with Weak Supervision. *arXiv preprint arXiv:2205.10203* (2022).
 - [7] Fangzhou Hong, Mingyuan Zhang, Liang Pan, Zhongang Cai, Lei Yang, and Ziwei Liu. 2022. AvatarCLIP: Zero-Shot Text-Driven Generation and Animation of 3D Avatars. *arXiv preprint arXiv:2205.08535* (2022).
 - [8] Meng-Ru Hsieh, Yen-Liang Lin, and Winston H Hsu. 2017. Drone-based object counting by spatially regularized regional proposal network. In *Proceedings of the IEEE international conference on computer vision*. 4145–4153.
 - [9] Chao Jia, Yinfei Yang, Ye Xia, Yi-Ting Chen, Zarana Parekh, Hieu Pham, Quoc Le, Yun-Hsuan Sung, Zhen Li, and Tom Duerig. 2021. Scaling up visual and vision-language representation learning with noisy text supervision. In *International Conference on Machine Learning*. PMLR, 4904–4916.
 - [10] Menglin Jia, Luming Tang, Bor-Chun Chen, Claire Cardie, Serge Belongie, Bharath Hariharan, and Ser-Nam Lim. 2022. Visual prompt tuning. *arXiv preprint arXiv:2203.12119* (2022).
 - [11] Haopeng Li, Lingbo Liu, Kunlin Yang, Shinan Liu, Junyu Gao, Bin Zhao, Rui Zhang, and Jun Hou. 2022. Video Crowd Localization With Multifocus Gaussian Neighborhood Attention and a Large-Scale Benchmark. *IEEE Transactions on Image Processing* 31 (2022), 6032–6047.
 - [12] Junnan Li, Dongxu Li, Caiming Xiong, and Steven Hoi. 2022. Blip: Bootstrapping language-image pre-training for unified vision-language understanding and generation. In *International Conference on Machine Learning*. PMLR, 12888–12900.
 - [13] Yanghao Li, Hanzhi Mao, Ross Girshick, and Kaiming He. 2022. Exploring plain vision transformer backbones for object detection. In *Computer Vision—ECCV 2022: 17th European Conference, Tel Aviv, Israel, October 23–27, 2022, Proceedings, Part IX*. Springer, 280–296.
 - [14] Dingkang Liang, Jiahao Xie, Zhikang Zou, Xiaoqing Ye, Wei Xu, and Xiang Bai. 2023. CrowdCLIP: Unsupervised Crowd Counting via Vision-Language Model. *arXiv preprint arXiv:2304.04231* (2023).
 - [15] Hui Lin, Xiaopeng Hong, and Yabin Wang. 2021. Object Counting: You Only Need to Look at One. *arXiv preprint arXiv:2112.05993* (2021).
 - [16] Jiayi Lin and Shaogang Gong. 2023. GridCLIP: One-Stage Object Detection by Grid-Level CLIP Representation Learning. *arXiv preprint arXiv:2303.09252* (2023).
 - [17] Wei Lin, Kunlin Yang, Xinzhu Ma, Junyu Gao, Lingbo Liu, Shinan Liu, Jun Hou, Shuai Yi, and Antoni B Chan. 2022. Scale-Prior Deformable Convolution for Exemplar-Guided Class-Agnostic Counting. (2022).
 - [18] Chang Liu, Yujie Zhong, Andrew Zisserman, and Weidi Xie. 2022. Countr: Transformer-based generalised visual counting. *arXiv preprint arXiv:2208.13721* (2022).
 - [19] Lingbo Liu, Jiaqi Chen, Hefeng Wu, Tianshui Chen, Guanbin Li, and Liang Lin. 2020. Efficient crowd counting via structured knowledge transfer. In *Proceedings of the 28th ACM international conference on multimedia*. 2645–2654.
 - [20] Lingbo Liu, Jiaqi Chen, Hefeng Wu, Guanbin Li, Chenglong Li, and Liang Lin. 2021. Cross-modal collaborative representation learning and a large-scale rgbt benchmark for crowd counting. In *Proceedings of the IEEE/CVF conference on computer vision and pattern recognition*. 4823–4833.
 - [21] Lingbo Liu, Zhilin Qiu, Guanbin Li, Shufan Liu, Wanli Ouyang, and Liang Lin. 2019. Crowd counting with deep structured scale integration network. In *Proceedings of the IEEE/CVF international conference on computer vision*. 1774–1783.
 - [22] Lingbo Liu, Hongjun Wang, Guanbin Li, Wanli Ouyang, and Liang Lin. 2018. Crowd counting using deep recurrent spatial-aware network. In *Proceedings of the 27th International Joint Conference on Artificial Intelligence*. 849–855.
 - [23] Ilya Loshchilov and Frank Hutter. 2017. Decoupled weight decay regularization. *arXiv preprint arXiv:1711.05101* (2017).
 - [24] Erika Lu, Weidi Xie, and Andrew Zisserman. 2018. Class-agnostic counting. In *Asian conference on computer vision*. Springer, 669–684.
 - [25] Aaron van den Oord, Yazhe Li, and Oriol Vinyals. 2018. Representation learning with contrastive predictive coding. *arXiv preprint arXiv:1807.03748* (2018).
 - [26] Roni Paiss, Ariel Ephrat, Omer Tov, Shiran Zada, Inbar Mosseri, Michal Irani, and Tali Dekel. 2023. Teaching CLIP to Count to Ten. *arXiv preprint arXiv:2302.12066* (2023).
 - [27] Or Patashnik, Zongze Wu, Eli Shechtman, Daniel Cohen-Or, and Dani Lischinski. 2021. Styleclip: Text-driven manipulation of stylegan imagery. In *Proceedings of the IEEE/CVF International Conference on Computer Vision*. 2085–2094.
 - [28] Zhilin Qiu, Lingbo Liu, Guanbin Li, Qing Wang, Nong Xiao, and Liang Lin. 2019. Crowd counting via multi-view scale aggregation networks. In *2019 IEEE International Conference on Multimedia and Expo (ICME)*. IEEE, 1498–1503.
 - [29] Alec Radford, Jong Wook Kim, Chris Hallacy, Aditya Ramesh, Gabriel Goh, Sandhini Agarwal, Girish Sastry, Amanda Askell, Pamela Mishkin, Jack Clark, et al. 2021. Learning transferable visual models from natural language supervision. In *International Conference on Machine Learning*. PMLR, 8748–8763.
 - [30] Viresh Ranjan and Minh Hoai Nguyen. 2022. Exemplar free class agnostic counting. In *Proceedings of the Asian Conference on Computer Vision*. 3121–3137.
 - [31] Viresh Ranjan, Udbhav Sharma, Thu Nguyen, and Minh Hoai. 2021. Learning to count everything. In *Proceedings of the IEEE/CVF Conference on Computer Vision and Pattern Recognition*. 3394–3403.
 - [32] Yongming Rao, Wenliang Zhao, Guangyi Chen, Yansong Tang, Zheng Zhu, Guan Huang, Jie Zhou, and Jiwen Lu. 2022. Densclip: Language-guided dense prediction with context-aware prompting. In *Proceedings of the IEEE/CVF Conference on Computer Vision and Pattern Recognition*. 18082–18091.
 - [33] Aditya Sanghi, Hang Chu, Joseph G Lambourne, Ye Wang, Chin-Yi Cheng, Marco Fumero, and Kamal Rahimi Malekshian. 2022. Clip-forgo: Towards zero-shot text-to-shape generation. In *Proceedings of the IEEE/CVF Conference on Computer Vision and Pattern Recognition*. 18603–18613.
 - [34] Min Shi, Hao Lu, Chen Feng, Chengxin Liu, and Zhiguo Cao. 2022. Represent, Compare, and Learn: A Similarity-Aware Framework for Class-Agnostic Counting. In *Proceedings of the IEEE/CVF Conference on Computer Vision and Pattern Recognition*. 9529–9538.
 - [35] Vishwanath A Sindagi and Vishal M Patel. 2017. Generating high-quality crowd density maps using contextual pyramid cnns. In *Proceedings of the IEEE international conference on computer vision*. 1861–1870.
 - [36] Can Wang, Ruixiang Jiang, Menglei Chai, Mingming He, Dongdong Chen, and Jing Liao. 2022. NeRF-Art: Text-Driven Neural Radiance Fields Stylization. *arXiv preprint arXiv:2212.08070* (2022).
 - [37] Mingjie Wang, Yande Li, Jun Zhou, Graham W Taylor, and Minglun Gong. 2023. GCNet: Probing Self-Similarity Learning for Generalized Counting Network. *arXiv preprint arXiv:2302.05132* (2023).
 - [38] Zhaoqing Wang, Yu Lu, Qiang Li, Xunqiang Tao, Yandong Guo, Mingming Gong, and Tongliang Liu. 2022. Cris: Clip-driven referring image segmentation. In *Proceedings of the IEEE/CVF conference on computer vision and pattern recognition*. 11686–11695.
 - [39] Zhengtao Wu, Lingbo Liu, Yang Zhang, Mingzhi Mao, Liang Lin, and Guanbin Li. 2022. Multimodal Crowd Counting with Mutual Attention Transformers. In *IEEE International Conference on Multimedia and Expo*. IEEE, 1–6.
 - [40] Jingyi Xu, Hieu Le, Vu Nguyen, Viresh Ranjan, and Dimitris Samaras. 2023. Zero-shot Object Counting. *arXiv preprint arXiv:2303.02001* (2023).
 - [41] Shuo-Diao Yang, Hung-Ting Su, Winston H Hsu, and Wen-Chin Chen. 2021. Class-agnostic few-shot object counting. In *Proceedings of the IEEE/CVF Winter Conference on Applications of Computer Vision*. 870–878.
 - [42] Zhiyuan You, Kai Yang, Wenhan Luo, Xin Lu, Lei Cui, and Xinyi Le. 2023. Few-shot object counting with similarity-aware feature enhancement. In *Proceedings of the IEEE/CVF Winter Conference on Applications of Computer Vision*. 6315–6324.
 - [43] Lixian Yuan, Zhilin Qiu, Lingbo Liu, Hefeng Wu, Tianshui Chen, Pei Chen, and Liang Lin. 2020. Crowd counting via scale-communicative aggregation networks. *Neurocomputing* 409 (2020), 420–430.
 - [44] Renrui Zhang, Ziyu Guo, Wei Zhang, Kunchang Li, Xupeng Miao, Bin Cui, Yu Qiao, Peng Gao, and Hongsheng Li. 2022. Pointclip: Point cloud understanding by clip. In *Proceedings of the IEEE/CVF Conference on Computer Vision and Pattern Recognition*. 8552–8562.
 - [45] Shanghang Zhang, Guanghan Wu, Joao P Costeira, and José MF Moura. 2017. Fcn-rlstm: Deep spatio-temporal neural networks for vehicle counting in city cameras. In *Proceedings of the IEEE international conference on computer vision*. 3667–3676.
 - [46] Yingying Zhang, Desen Zhou, Siqin Chen, Shenghua Gao, and Yi Ma. 2016. Single-image crowd counting via multi-column convolutional neural network. In *Proceedings of the IEEE conference on computer vision and pattern recognition*. 589–597.
 - [47] Yiwu Zhong, Jianwei Yang, Pengchuan Zhang, Chunyuan Li, Noel Codella, Liunian Harold Li, Luowei Zhou, Xiyang Dai, Lu Yuan, Yin Li, et al. 2022. Regionclip: Region-based language-image pretraining. In *Proceedings of the IEEE/CVF Conference on Computer Vision and Pattern Recognition*. 16793–16803.
 - [48] Kaiyang Zhou, Jingkang Yang, Chen Change Loy, and Ziwei Liu. 2022. Conditional prompt learning for vision-language models. In *Proceedings of the IEEE/CVF Conference on Computer Vision and Pattern Recognition*. 16816–16825.
 - [49] Kaiyang Zhou, Jingkang Yang, Chen Change Loy, and Ziwei Liu. 2022. Learning to prompt for vision-language models. *International Journal of Computer Vision* 130, 9 (2022), 2337–2348.
 - [50] Ziqin Zhou, Bowen Zhang, Yinjie Lei, Lingqiao Liu, and Yifan Liu. 2022. ZegCLIP: Towards Adapting CLIP for Zero-shot Semantic Segmentation. *arXiv preprint arXiv:2212.03588* (2022).